Acta Physica Universitatis Comenianae
Vol. XLVI–XLVII, (2005–2006) 39–51

# Studies of Structure and Growth of Metal Oxide Clusters in Gas Phase

V. Foltin

Department of Experimental Physics, Faculty of Mathematics, Physics and Informatics, Comenius University, Mlynská dolina F2, 842 48 Bratislava, Slovak Republic, e-mail: *vfoltin@fmph.uniba.sk*

**Abstract:** Metal oxide clusters are often considered to be a promising medium that may help study fundamental principles of heterogeneous catalysis on the molecular level. To enable studies and interpretation of cluster size selective reactivity of these systems, one must first learn how to control cluster growth and composition and to understand correlation between the cluster size and structure. In this article we will review interesting prior studies and supplement them with new data of how the supersonic expansion and time of flight mass spectrometry techniques in combination with simple kinetic growth modeling and molecular orbital calculations can be used to help control the cluster growth and understand the cluster structure.

## 1. Introduction

One could hardly imagine a wide variety of processes in the modern world without catalysis. Many processes involved in fuel conversion, synthesis of complex chemicals and polymers from simpler chemicals, and in exhaust purification, are made possible or less energy demanding using advanced catalysts. A better understanding of the fundamental principles of catalysis on the molecular level may help to create more efficient new catalyst materials. Heterogeneous catalysts are multifunctional materials composed of several active components and a high-surface-area support material. Therefore, the compositional parameter space associated with them is very large. In addition, one also needs to consider a wide variety of parameters related to the method of preparation, as well as reaction conditions to which a given catalyst could be subjected. This increases the total number of possible experimental contributions even more.

Early transition metal oxides are used as supports for metal catalysts and in many cases they are found to be active catalysts themselves. For example, a vanadium oxide catalyst is used for catalytic oxidation of $SO_2$ to $SO_3$ which is an important step in production of sulfuric acid [1]. Titanium oxide catalyst has been found to photo-oxidize CO, $C_3F_6$, and $CH_3Cl$ to different sets of products depending on oxide surface structure [2]. Metal oxides play an important role in methanol synthesis from methane (which is known to be a candidate to replace presently used fuels) [2, 3], propylene oxidation [4] and the reduction of NO to $N_2$ [5]. The detailed microscopic properties of the active sites in such reactions are not very well known. One path to elucidating the electronic structure and details of catalytically active materials is through cluster studies. Surfaces of finely divided metal oxide powders have complicated morphologies consisting of various crystallographic planes, grain structures, and grain interfaces. Clusters of metal oxides formed in the gas phase, on

the other hand, have relatively well-defined structures that vary systematically with cluster size. Some cluster geometries can mimic particular defect structures on metal oxide surfaces. For example, it has been suggested that the partial oxidation of methane on magnesium oxide catalysts occurs primarily on low-coordinated sites $Mg_{3C}$ $O_{3C}$, $Mg_{3C}$ $O_{4C}$, $Mg_{4C}$ $O_{3C}$ and $Mg_{4C}$ $O_{4C}$ on various surface defects such as kinks, terraces, corners, etc. The detailed role of these sites, however, is not very well known. It is difficult to prepare surfaces with well defined distributions of these sites for detailed experimental studies. In clusters, on the other hand, the number of $Mg_{3C}$ $O_{3C}$, $Mg_{3C}$ $O_{4C}$, $Mg_{4C}$ $O_{3C}$ and $Mg_{4C}$ $O_{4C}$ sites is a well understood function of the cluster size. Thus, gas phase clusters can represent a good model system for condensed phase properties and behavior. Metal oxide cluster properties, structures, reactivity, and catalytic efficacy should change with cluster size. Therefore, systematic exploration of properties, structure, and catalytic reactivity of neutral transition metal oxide clusters as a function of cluster size may be a promising technique for gaining better understanding at the molecular level of the practical application of metal oxide species in catalysis. A significant advantage of cluster studies over surface or condense phase studies is that clusters can be isolated in the gas phase and thus, they are amenable to individual access both experimentally and theoretically.

The first steps towards making this technique useful are: i) to be able to understand and control the cluster growth so that the ensuing cluster distribution contains sufficient cluster concentrations for those cluster compositions and sizes that are most relevant for catalytic reactivity studies, and, ii) to be able to understand correlation between the cluster size and cluster structures. This article will review interesting prior studies and supplement them with new data to show methods how to achieve these two goals. The metal oxide clusters are typically produced by laser ablation of metal or metal oxide target into a flow of He or Ar/He carrier gas mixed with small amount of $O_2$ or $N_2O$, although other techniques have also been used that employ pulsed arc discharge, ion surface sputtering or pyrolysis of metal-organic precursor. In this paper we show how correlations of fluctuations between cluster signal intensities from various cluster compositions and cluster sizes in the mass spectrum can be interpreted with the aid of simple cluster growth kinetic model to give insights to the dynamics of metal oxide cluster growth in laser plasmas. As examples, we will discuss growth of vanadium oxide and mixed vanadium oxide – vanadium nitride clusters studied at Colorado State University in the laboratory of Prof. Elliot Bernstein. Once the cluster growth dynamic is understood and can be controlled, the second requirement for successful catalytic activity studies is to understand the cluster structure trends as function of cluster size. In our previous article [6] we described LIF spectroscopy method applied to structure studies of small organic clusters. Unfortunately, since small metal oxide particles ($M_xO_y$, 1 $x, y$ 100) have typically an enormous density of vibronic states and thus, poorly resolved spectra and very rapid relaxation processes, they cannot be studied by the LIF. Their study and characterization is typically through mass spectroscopy [7]. We will show how occurrence of "magic" number, i.e., of a cluster size with exceptionally strong intensity in mass spectrum can be interpreted with the aid of molecular orbital calculations technique for zirconium oxide cluster and how the trend in mass spectral intensities observed over several cluster sizes with several "magic" and "anti-magic" numbers can be used to predict structures of vanadium sulfide clusters.

## 2. Experiment

The experimental setup consisting of a laser ablation cluster source, the reaction cell and a time-of-flight mass spectrometer (see Fig. 1) has been described in detail in references [8 11].

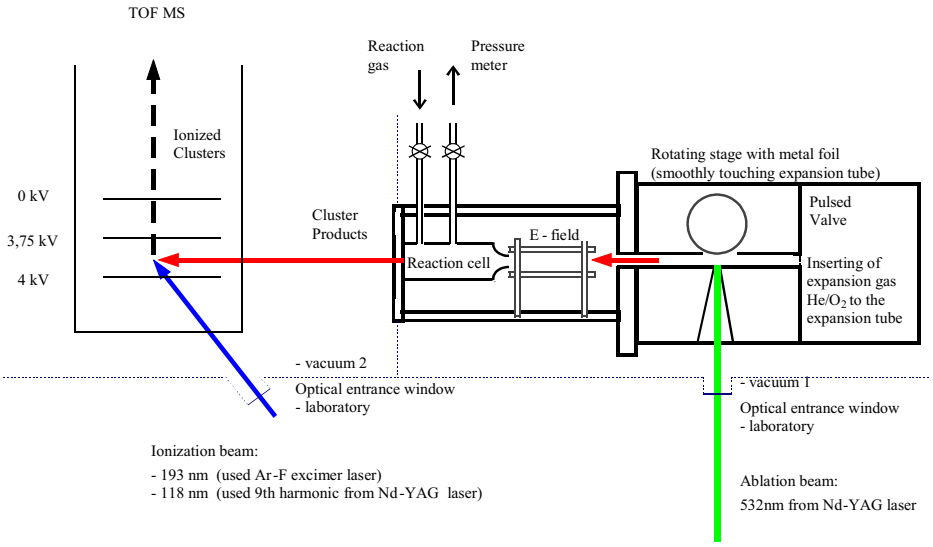


**Fig. 1.** Experimental set up.

Neutral metal oxide clusters are produced by laser ablation technique using 532 nm pulsed laser beam ($2^{nd}$ harmonic from Nd YAG laser) focused on a surface of a metal foil placed on a rotating stage. The surface of the foil is checked after the experiment by an optical microscope to verify that the ablation laser beam did not drill a hole in the foil. The metal plasma plume from the ablation process interacts with the carrier gas, typically 1 % $O_2$/ 99 % He at a pressure of several atmospheres, that passes over the ablation point through a narrow channel at right angle with respect to the laser beam. The oxidation and cooling of the metal vapor in the plasma plume that is expanding from the surface and interacting with the carrier gas leads to generation of $M_mO_n$ clusters. The carrier gas is injected to the cluster source through a pulse valve and the timing of the ablation laser pulse with respect to the gas pulse can be varied to study effects of ablation at different times of the gas pulse (i.e., on the pulse front, where the gas pressure is lower, or on the pulse center, where the pressure is higher). The carrier gas/cluster mixture expands from the cluster source to vacuum by supersonic expansion (leading to further cooling of the clusters) and the ensuing cluster beam then passes through an electric field directed perpendicularly to the cluster beam to deflect ionized clusters away from the beam. After passing the deflection field, the neutral clusters enter a reaction cell that can contain reaction gas at a pressure of several mTorr. The reaction cell allows studying interaction of clusters with various reactant molecules or it can simply be kept evacuated for studies of cluster growth and structure. The cluster beam then passes from the reaction cell to a differentially pumped time-of-flight mass spectrometer (TOFMS). In the

spectrometer, the neutral clusters are ionized by multiphoton ionization with 193 nm beam from ArF pulsed excimer laser and the cluster ions produced in this way are extracted at right angle by strong electric field to the flight tube of the spectrometer. In the flight tube, the cluster ions from the laser pulse are separated in time based on their mass and detected by a multi-channel plate detector (MCP). The time delays between the gas pulse, the ablation laser pulse and the ionization laser pulse are set by timing box from Stanford Research Instruments and the ion signal from the MCP detector is fed to a digital storage oscilloscope with time resolution of 4 ns per channel (or better) and capacity of 16000 channels or better. The lasers and the pulse valve operate at 10 Hz frequency and the signal trace from the oscilloscope is sent to a PC computer between each successive pulses for real time signal processing that includes computation of covariance map between the mass channels as well as the average value in each channel. The recording of spectra and covariance maps is typically done over 1000–10000 pulses. To minimize the neutral cluster fragmentation in the ion source of the mass spectrometer, instead of using the multi-photon ionization by rather intense (~1 50 mJ/pulse) ArF laser beam at 193 nm, one can also employ a single-photon ionization using a weak 118 nm beam produced by frequency tripling the 355 nm output from Nd YAG laser in a static gas cell filled with Xe/Ar gas mixtures (~1:10) at 200 Torr (Fig. 2). Note that the 118 (10.5 eV) photons have energy high enough to ionize metal oxide neutral clusters by a single photon ionization and at $10^{11}$ $10^{12}$ photons/pulse at 118 nm the probability that any cluster would absorb more than one photon is negligible [12]. Conversely, the 193 nm (6.4 eV) photons from ArF laser are not high enough in energy for a single photon ionization and, consequently, higher laser intensities need to be used to allow two-photon ionization, which also increases the possibility of cluster fragmentation upon absorption of further (third, etc.) photon. A careful study of the dependence of cluster signal intensity on laser beam intensity is then necessary to help set the laser intensity low enough to prevent excessive fragmentation.

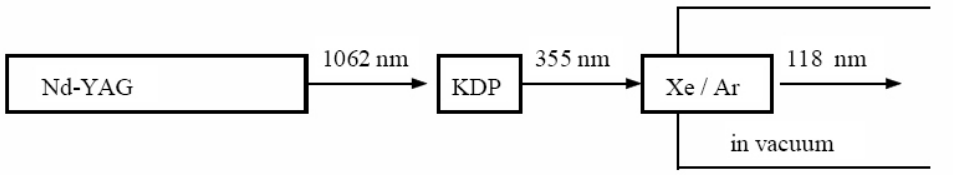


**Fig. 2.** Schematic view of 118 nm laser beam generation.

## 3. Results and Discussion

### *3.1. Cluster growth*

We will report here on studies of cluster growth dynamics of vanadium oxide and mixed vanadium oxide – vanadium nitride clusters. The vanadium oxide studies are based on the data from Ref. [8]. The mixed vanadium oxide – vanadium nitride studies are reported for the first time in this paper. The mass distribution of vanadium oxide clusters

shows two different components – the oxygen rich and oxygen poor (see Fig. 3). Both components coexist in the mass spectrum when the ablation laser beam is fired close to the front of the gas pulse from the pulse nozzle. The oxygen poor component decreases in intensity at high ablation laser powers and increases in intensity upon lowering the nozzle current (i.e., decreasing the carrier gas concentration). This component can disappear from the mass spectrum when the laser beam is fired in the center of the gas pulse from the pulse nozzle where the carrier gas concentration is high.

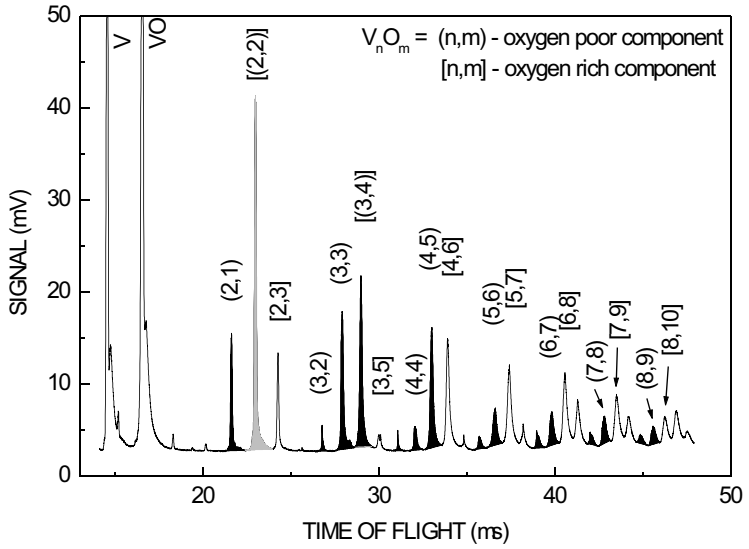


**Fig. 3.** Mass spectrum of $V_nO_m$ clusters [8]. The cluster peaks in the oxygen poor component are filled black. The cluster peaks in the oxygen rich component are unfilled. The $V_2O_2$ peak is on the overlap between the two components.

The technique of covariance mapping was employed to measure correlations between pulse-to-pulse fluctuations of signal intensities in different mass peaks. In this technique, the mass spectra are collected over $n = 2500$ laser pulses and for each laser pulse $i$ a separate time-of-flight mass spectrum is captured (instead of just capturing the average over all $n$ pulses). The set of $n$ mass spectra collected in this way is then used to calculate covariance between any two mass spectral peaks x and y to measure the extent of correlated fluctuations of signal intensities in these peaks using formula:

$$\text{Covariance}\,(x, y) \quad \frac{1}{n}\sum_{i=1}^{n}(x_i - \bar{x})(y_i - \bar{y})$$

$$\text{where}\ \bar{x} \quad \frac{1}{n}\sum_{i=1}^{n} x_i\,, \qquad \bar{y} \quad \frac{1}{n}\sum_{i=1}^{n} y_i$$

where $x_i$, $y_i$ are the signal intensities in peaks x and y, respectively, in laser pulse *i*. The covariance is then normalized by dividing the covariance values with the product of average signal intensities $\bar{x}\ \bar{y}$.

The covariance mapping shows that the oxygen rich and the oxygen poor components grow independently on each other – they are weakly correlated. Different peaks within the oxygen poor component show a strong covariance between each other. The covariance is strong not only between the neighbouring cluster sizes in this component, but also between clusters that are many cluster sizes apart (see Fig. 4).

| $X_n$ | 2 | 3 | 4 | 5 | 6 | 7 |
|---|---|---|---|---|---|---|
| 2 | 77±14 | 60±13 | 66±13 | 60±15 | 58±15 | 54±15 |
| 3 | 60±13 | 65±15 | 65±14 | 59±16 | 57±15 | 51±15 |
| 4 | 66±13 | 65±14 | 94±17 | 67±16 | 66±16 | 63±16 |
| 5 | 60±15 | 59±16 | 67±16 | 69±18 | 61±17 | 58±17 |
| 6 | 58±15 | 57±15 | 66±16 | 61±17 | 69±18 | 60±17 |
| 7 | 54±15 | 51±15 | 63±16 | 58±17 | 60±17 | 65±17 |

**Fig. 4.** Measured covariance table for the oxygen poor component of $V_nO_m$ mass spectrum. Covariance values normalized by division with the product of average signal intensities are shown, multiplied by factor 1000 to improve readability of the table.

High covariances (0.048–0.067) within the oxygen weak component mean that i) the pulse-to-pulse signal intensity fluctuations of individual peaks within this component are high (i.e., they have high variance), and, ii) the fluctuations between different peaks within this component are highly correlated (i.e., high correlation coefficient). Different peaks in the oxygen rich component show medium size covariances (0.028–0.038) – these peaks are still correlated between each other in a similar manner like peaks within the oxygen poor component, but their pulse-to-pulse fluctuations are much smaller. As emphasized above, these peaks are only very weakly correlated with the independent oxygen poor contribution.

To perform cluster growth modeling, we will focus now on the oxygen poor component (the interpretation is similar for the oxygen rich component). The interesting observation is that the covariance is strong not only between the neighbouring cluster sizes but also between clusters that are many cluster sizes apart. To explain this covariance pattern, a simple sequential growth kinetic model was considered (see Fig. 5). In this model, the cluster dimer growth rate was allowed to fluctuate at different rate than the larger clusters growth rate, which was assumed to scale proportionally to the cluster cross-section.

It was found that the measured covariance pattern cannot be explained by allowing large fluctuations of the large clusters growth rate. This would lead to simulated covariance pattern where the covariance between the neighboring cluster sizes was much higher than that between clusters that are many cluster sizes apart. However, the measured covariance pattern was matched reasonably well with simulation by allowing large fluctuations of the dimer growth rate.

These observations lead to the following interpretation. The dimer formation is the kinetic bottleneck for formation of large clusters. Once the dimer is formed, the addition of further $VO_2$ or VO constituents (in a series of collisions of the cluster with the $VO_2$ or VO molecules and the carrier gas atoms to remove the excess energy) is a relatively stable pro-

**Simple cluster growth model:**

$$\frac{d\langle X_n\rangle}{dt} = \frac{K_{n-1}\langle X_{n-1}\rangle}{t^2} - \frac{K_n\langle X_n\rangle}{t^2}$$

where:

$$X_n = V_nO_m$$

$$K_1 = k_d \frac{[VO]\alpha d^2}{v^2}$$

$$K_n = k_c n^{0.66} \frac{[VO]\alpha d^2}{v^2} = K_c n^{0.66}$$

$k_d$ : $V_2O_2$ dimer formation rate constant
$k_c n^{0.66}$ : $V_{n+1}O_{m+1}$ cluster formation rate constant
d : ablation spot diameter
v : plume expansion velocity
$\alpha$ : geometric factor

**Parameters of simulation:**

$K_c/t_0$ : normalized cluster growth rate ($t_0$ is time when cluster growth starts)
$k_d/k_c$ : dimer formation rate relative to rate of larger cluster growth

**Best fit to the measured mass spectrum:**
$K_c/t_0 = 1.9$, $k_d/k_c = 0.1$

**Fig. 5.** Simple cluster growth model $V_nO_m$ clusters.

cess. In oxygen weak clusters, the pulse-to-pulse dimer fluctuations are large, leading to large correlated fluctuation between all the cluster sizes in this component. It is possible that the oxygen poor clusters are formed on the periphery of the ablation plasma plume where the temperature is lower and the temperature and metal density fluctuate more. In oxygen rich clusters, the pulse-to-pulse dimer fluctuations are smaller, leading to smaller correlated fluctuations between all cluster size and therefore to medium size covariances in this component.

This shows that the resulting cluster distribution has multiple components and one can enhance some components and weaken other by a careful adjustment of the conditions in the ablation laser plume. It also shows that the production of very small clusters (dimers) may be determining the stoichiometry of the whole distribution.

We extended this to cluster growth studies of mixed vanadium oxide – vanadium nitride clusters. These were produced by admixing small amount of ammonia (~ 3 %) to the He carrier gas flow that also contained about 1 % of $O_2$. The mass spectrum is shown in Fig. 6.

One question here is whether these clusters form nitroxide (NO) type compounds where nitrogen is coordinated to oxygen or whether the nitrogen is coordinated to vanadium like in vanadium nitrides. The spectrum indicates that the latter is the case. Notice that, for example, for n = 2, the distribution contains V, VO, $VO_2$, $V_2O$, $V_2N$, $V_2ON$, $V_2O_2$, $V_2O_2N$, $V_2O_3$, $V_2O_4$ and $V_2O_5$ but not $VO_3$, $VO_4$, $VO_5$, $V_2O_3N$, $V_2O_4N$ and $V_2O_5N$. Basically, for each $V_nO_m$ present in the distribution, $V_{n+1}O_mN$ is also present, and for each $V_nO_m$ absent in the distribution, $V_{n+1}O_mN$ is also absent. This pattern suggests that the $V_2O_nN$ dimer clusters are produced by addition of VN to V, VO, $VO_2$ and the $V_2O_n$ dimer clusters are produced by addition of mostly VO and $VO_2$ to V, VO, $VO_2$ (the exception to

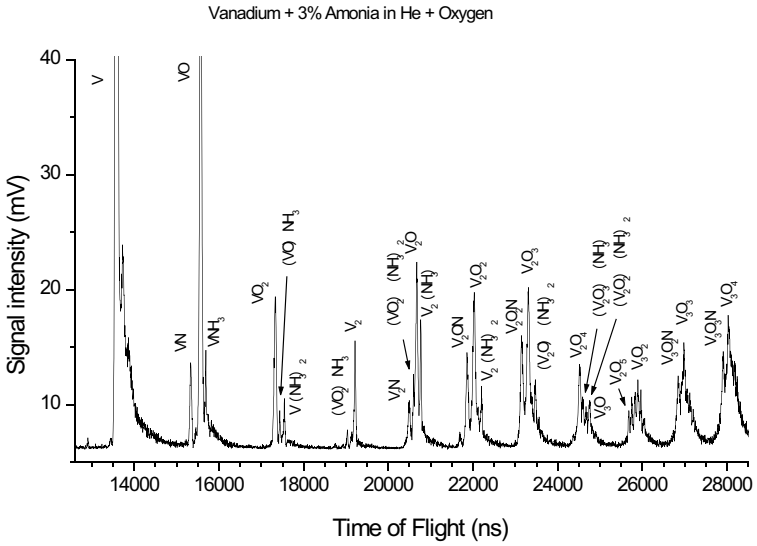


**Fig. 6.** Mass spectrum of $V_nO_mN_p$ clusters.

this pattern is the thermodynamically very stable $V_2O_5$ that appears in the spectrum in very low quantities despite that no $VO_3$ is in the spectrum).

Note that the spectrum also contains $V_nO_m(NH_3)$ and $V_nO_m(NH_3)_2$ clusters. Careful studies of cluster signal intensity as function of ionization laser intensity will be carried out in the future to see how strongly are the $NH_3$ adducts bonded to the $V_nO_m$ clusters (i.e., whether they are physisorbed or chemisorbed). Since the chemisorption is the important first step needed to open possible catalytic reaction channels, this may give some initial insights into the propensity of these clusters to possible catalytic activity as function of the cluster size.

### *3.2. Cluster structures*

We will report here on studies of cluster structure of zirconium-oxide and vanadium sulfide clusters. The zirconium oxide studies are based on the data from Ref. [9]. The vanadium sulfide studies are reported for the first time in this paper.

The mass spectrum of zirconium oxide clusters consists primarily of $(ZrO_2)_n$ clusters, consistently with zirconium oxidation number 4, although the clusters with one less oxygen and one or two more oxygen atoms are also present with lower intensities. Notably, the intensity of $(ZrO_2)_5$ cluster peak is much stronger than intensities of its neighbours, $(ZrO_2)_4$ and $(ZrO_2)_6$. The cluster size n = 5 is a "magic" number.

Careful study of mass spectral signal intensity as a function of ionization laser intensity reveals that the $(ZrO_2)_5$ cluster undergoes absorption of two to three photons at 193 nm (6.4 eV photon energy) in the ionization process. Assuming cluster ionization energy of around 8 eV and dissociation energy of around 4 eV, simple calculation using RRK

unimolecular dissociation theory shows that the energy deposited by the absorption of two to three photons is not enough to cause significant cluster fragmentation on the microsecond time scale (i.e., in the cluster source of the mass spectrometer). Furthermore, as the laser intensity is reduced from 0.5 mJ to 0.2 mJ, the $(ZrO_2)_5$ still remains the "magic" number (see Fig. 7). This suggests that the $(ZrO_2)_5$ magic character in the mass spectrum is due to the $(ZrO_2)_5$ neutral cluster stability rather than due to the $(ZrO_2)_5^+$ cluster ion stability against the fragmentation in the ion source of the mass spectrometer.

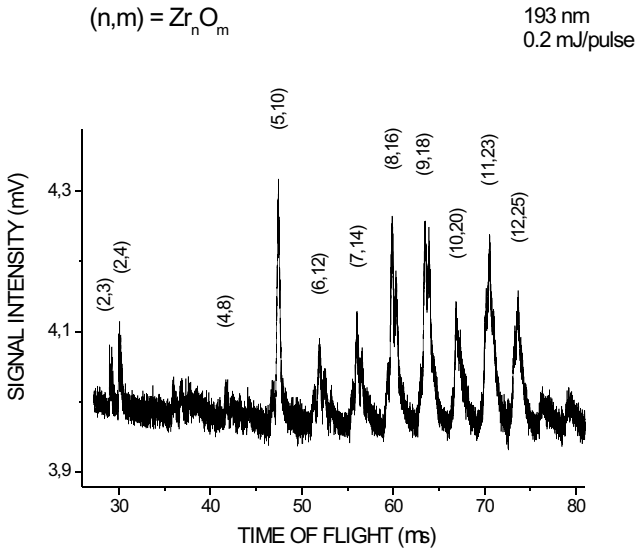


**Fig. 7.** Mass spectrum of $Zr_nO_m$ clusters.

The reasons for the unusual stability of $(ZrO_2)_5$ have been studied using molecular orbital calculations of cluster structure with the aid of Density Functional Theory (DFT). Two different methods and basis sets have been used. The first method uses Gaussian basis set with double zeta valence functions and effective core potential functions for Zr atom and full double zeta functions for O atom. The second method places the cluster in a supercell that repeats in space and uses linear (Bloch) functions, cut-off energy of about 380 eV, and ultra soft pseudo-potentials for the core wavefunctions to give reasonable account for the effects of the core electrons. The advantage of using linear periodic Bloch functions is the significant reduction in computation time for overlap integrals. The downside is that the supercell, which encapsulates the cluster, repeats in space to form a three-dimensional lattice with lattice constant related to supercell size. Therefore, the size of the supercell was selected to be large enough to minimize interaction of the cluster with the neighboring clusters in the adjacent projections of the supercell. The geometry optimizations were carried out with full relaxation of all coordinates, starting from several reasonable initial structures for each cluster size.

The calculation with both techniques reveals that the most stable structures of $(ZrO_2)_4$, $(ZrO_2)_5$ and $(ZrO_2)_6$ are those shown in Fig. 8. Each cluster size has also several other isomer structures, but these are at least 0.15 eV less stable than the most stable structures shown in Fig. 8.

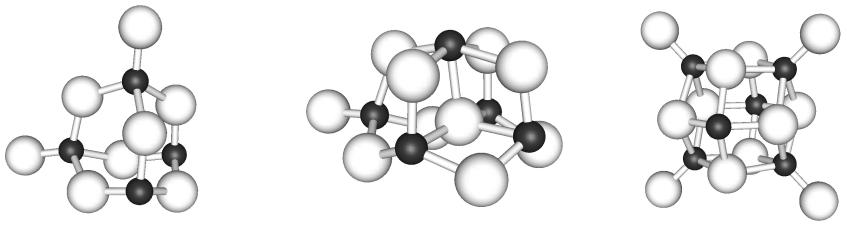

**Fig. 8.** Calculated structures of $(ZrO_2)_4$, $(ZrO_2)_5$ and $(ZrO_2)_6$ clusters. (Zr = small black balls, O = big gray balls).

The adiabatic dissociation energy $E_d$ for reaction $X_n \rightarrow X_{n-1} + X_2$ is often used as a measure of stability of cluster $X_n$. Based on the above described molecular orbital calculations, the adiabatic dissociation energies $E_d$ computed from the formula: $E_d = E_{n-1} + E_1 - E_n$, where $E_{n-1}$ is the total energy of $(ZrO_2)_{n-1}$ cluster, $E_1$ is the total energy of $ZrO_2$ and $E_n$ is the total energy of $(ZrO_2)_n$ cluster, are 5.6, 6.1 and 4.3 eV, for cluster sizes n = 4, 5 and 6, respectively. This is consistent with the experimental observations that $(ZrO_2)_5$ is more stable than $(ZrO_2)_4$ and $(ZrO_2)_6$.

The agreement between the calculation and the experiment is significant – it shows that the calculation can be "calibrated" with the experimental data and that the selected basis functions for valence electrons and the effective core potentials for the core electrons give a good agreement with the experiment. One can now extend these calculations to make predictions or gain better understanding about size-dependent reactivity trends of these clusters. This will be the subject of the future study. For example, the structures showed in Fig. 8 themselves show interesting trends in oxygen coordination that may impact reactivity. The cluster size n = 4 has two low coordinated oxygen atoms while cluster size n = 5 has only one low coordinated oxygen atom and cluster size n = 6 has four low coordinated oxygen atoms in the most stable isomer. The low coordinated oxygen atoms are in general weaker bound to the cluster and are more prone to removal from the cluster in reactions with CO and $H_2$. The reduction (i.e., oxygen removal) from zirconium oxide is an issue in industrial applications. For example, zirconium oxide coatings are used as heat barrier liners in combustion chambers of jet engines and coal fired electric power plants. The deterioration of these coatings because of $H_2$ and CO presence in combustion gases is a serious cost issue. These clusters may provide opportunity to study the role of oxygen coordination and low coordinated oxygen sites in the reduction process and help to design coatings with better morphologies that avoid the most reactive sites. The correlation between the cluster

size and the oxygen atom coordination established in Ref. 9 and here is the first step to enable such studies.

We also studied the structures of vanadium sulfide clusters. The mass spectrum of vanadium sulfide oxide clusters consists primarily of $(VS)_n$ clusters, suggesting that the oxidation number of vanadium in these clusters is 2 (see Fig. 9), i.e., each vanadium atom contributes two valence electrons to the cluster bond. Note that this is different from the solid state vanadium sulfide which usually occurs with oxidation numbers 3 (as $V_2S_3$) and 4 (as $VS_2$).

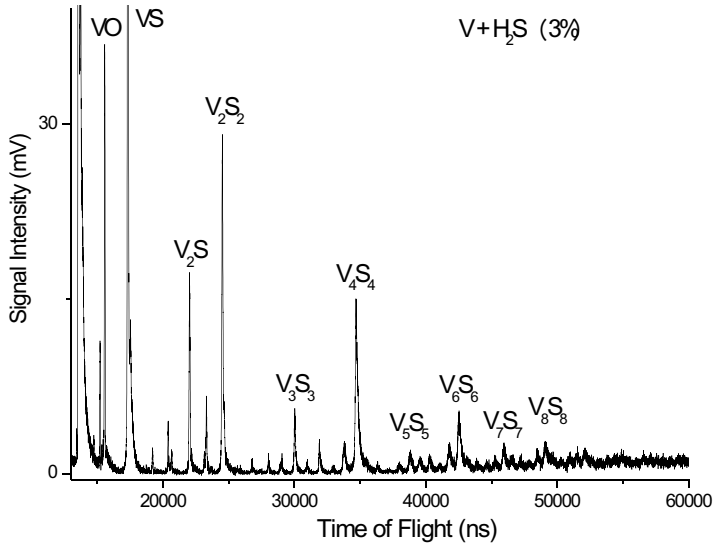


**Fig. 9.** Mass spectrum of vanadium-sulfide clusters.

The mass spectrum shows intensity maxima ("magic numbers") at cluster sizes n = 2, 4 and 6, and minima ("anti-magic numbers") at cluster sizes n = 3 and 5. This magic number pattern corresponds to cubic (i.e., rock-salt like) cluster structures. The n = 4 cluster is very stable because each vanadium and sulfur atom is coordinated to three sulfur and vanadium neighbours, respectively, in a 2 2 2 cube. The n = 5 cluster is less stable because it contains a VS adduct attached to the cube, where the V and S atoms are coordinated to only two neighbouring sulfur and vanadium atoms. The n = 6 is very stable again – it corresponds to 3 2 2 cubic slab where all corner atoms are three-coordinated and the edge atoms are four-coordinated. The n = 7 cluster is less stable because it again contains a VS adduct with two-coordinated V and S atoms. Under the current experimental conditions, the mass spectral intensities decrease rapidly with the increasing cluster size. Future studies will be carried out with the experimental conditions optimized for the production of larger clusters to check if the larger clusters also follow this cubic pattern. Note that there is some analogy here with vanadium (II) oxide solid phase that is known to have cubic structures. The interesting part about cubic clusters is that the ratio between four coordi-

nated (edge) VS sites and three coordinated (corner) VS sites is increasing with cluster size. Therefore, if the larger clusters also follow the cubic pattern observed here for the small clusters, a comparison of reactivity between the large and the small clusters may give insights to the reactivity differences between three-coordinated and four-coordinated sites. Furthermore, the less stable clusters with two-coordinated sites may show different reaction pattern.

## 4. Conclusions

In this work we have shown examples of some methods to study growth dynamics and structure of clusters of various metal compounds (oxides, nitrides, sulfides, etc.). We showed results of cluster growth studies of vanadium oxide and mixed vanadium oxide – vanadium nitride clusters and results of cluster structure studies of zirconium oxide and vanadium sulfide clusters. As we explained in the introduction, clusters may serve as models for catalytically active defect sites on solid surfaces. The ability to generate and interrogate these clusters in isolation from outside environment is attractive. However, this isolation also complicates the cluster studies – for example, one cannot use crystallographic techniques to study cluster structures. Different experimental methods have to be employed. In this paper we have shown that one can get insights into the cluster growth dynamic using mass spectrometry in combination with covariance mapping technique. This can help better optimize cluster generation conditions. We observed two independent components in the growth pattern of vanadium oxide clusters produced by laser ablation. The formation of the "dimer" ($V_2O$, $V_2O_2$ or $V_2O_3$) cluster "nucleus" is the rate determining factor in the cluster growth. Hence, if the observed cluster distribution is too broad, with multiple $V_nO_m$ stoichiometries for each cluster size n, one can focus on changing the "dimer" formation conditions to selectively eliminate the unwanted distribution component. This can be achieved by changing the oxygen concentration in the carrier gas and/or by changing the ablation laser power. We studied the mixed vanadium oxide – vanadium nitride clusters by admixing ammonia to the carrier gas and we found that these clusters likely grow by addition of VN to V, VO, $VO_2$ or larger vanadium oxide clusters. We also observed vanadium oxide clusters with one or two $NH_3$ adducts under these conditions and further studies will be needed to find out if ammonia is physisorbed or chemisorbed on $V_nO_m$ clusters. Ammonia can be a good probe for studying chemical binding propensity of clusters with different size that may have varying number of low coordinated, potentially catalytically active sites.

To study cluster structures, we demonstrated that one can use the "magic" numbers, i.e., cluster sizes with exceptionally high signal intensities in the mass spectrum and correspondingly high stabilities, to "calibrate" the molecular orbital calculations that can then be used to predict the cluster structures and coordination of surface sites. As an example we used the zirconium oxide clusters that show strong magic number $(ZrO_2)_5$. The molecular orbital calculations of these clusters correctly predicted the high stability of $(ZrO_2)_5$ as compared with $(ZrO_2)_4$ and $(ZrO_2)_6$, when using the Density Functional Theory approximation, double zeta Gaussian basis functions or Bloch linear wave functions for Zr valence electrons and effective core potentials for Zr core electrons. Interestingly, the calculations showed varying number of low coordinated oxygen atoms in the most stable

isomers in these clusters, which can potentially be employed in the future to study the role of oxygen coordination in the reduction process of zirconium, which is an issue in industrial applications. We also studied the structures of vanadium sulfide clusters. We found that small vanadium sulfide clusters have $(VS)_n$ stoichiometries with vanadium oxidation number 2. Based on the observed "magic number" patterns we concluded that these clusters have cubic (i.e., rock-salt like) structures. These structures have well defined progression of two-, three-, and four-coordinated VS sites as a function of cluster size. Future reaction studies of these clusters as a function of cluster size may help to understand what the relative chemical activities of these low-coordinated VS sites are.

## Acknowledgements

The author is grateful for the possibility to carry out the mixed vanadium oxide – vanadium nitride and the vanadium sulfide experiments during his stay in the laboratory of Prof. Elliot Bernstein at the Colorado State University. Help and discussions with Y. Matshuda, who has previously done similar experiments, and with Sen-Gui He, is also acknowledged. The experimental work at the Colorado State University has been supported by grant by Phillip Morris USA. The core of the presented paper was sponsored within the frame of the following Slovak projects: the Scientific Grant Agency of Slovak Republic VEGA 1/2014/05, 1/3043/06 by Slovak Ministry of Education Developing Project (RP) for 2005/2006 and by the Science and Technology Assistance Agency under the contract No. APVT-20-020204.

## References

[1] I. A. Fisher, A. T. Bell: J. Catal. **178** (1998) 153.
[2] R. A. Koppel, C. Stocker, A. Baiker, J. Catal. **179** (1998) 515.
[3] J. B. Reitz, E. I. Solomon: J. Am. Chem. Soc. **120** (1998) 11467.
[4] Y. J. Huang, H. P. Wang: J. Phys Chem. A **103** (1999) 6514.
[5] Y. Chi, S. S. C. Chuang: J. Catal. **190** (2000) 75.
[6] V. Foltin: Acta Physica Univ. Comeniane (Com. Univ. Press) **44 45** (1 2)(2004) 53 60.
[7] A. W. Castleman, Jr., K. H. Bowen, Jr.: J. Phys. Chem. **100** (1996) 12911.
[8] M. Foltin, G. J. Stueber, E. R. Bernstein: J. Chem. Phys. **111** (1999) 9577.
[9] M. Foltin, G. J. Stueber, E. R. Bernstein: J. Chem. Phys. **114** (2001) 871.
[10] Y. Matsuda, D. N. Shin, E. R. Bernstein: J. Chem. Phys. **120** (2004) 4142.
[11] D. N. Shin, Y. Matsuda, E. R. Bernstein: J. Chem. Phys. **120** (2004) 4150.
[12] D. N. Shin, Y. Matsuda, E. R. Bernstein: J. Chem. Phys. **120** (2004) 4157.
[13] Y. Matsuda, D. N. Shin, E. R. Bernstein: J. Chem. Phys. **120** (2004) 4165.